Dynamics and self-consistent chaos in a mean field Hamiltonian model

Diego del-Castillo-Negrete

Oak Ridge National Laboratory
Oak Ridge, TN 37831-8071, USA

Abstract. We study a mean field Hamiltonian model that describes the collective dynamics of marginally stable fluids and plasmas in the finite N and $N \to \infty$ kinetic limit (where N is the number of particles). The linear stability of equilibria in the kinetic model is studied as well as the initial value problem including Landau damping. Numerical simulations show the existence of coherent, rotating dipole states. We approximate the dipole as two macroparticles and show that the $N = 2$ limit has a family of rotating integrable solutions that provide an accurate description of the dynamics. We discuss the role of self-consistent Hamiltonian chaos in the formation of coherent structures, and discuss a mechanism of "violent" mixing caused by a self-consistent elliptic-hyperbolic bifurcation in phase space.

1 Introduction

The study of many-body interacting systems has been a problem of interest in science for many years. Examples of particular interest include plasmas, hydrodynamics, gravitational systems, and coupled dynamical systems. The dynamics of these systems is self-consistent in the sense that the evolution of a given member of the system is determined by the collective effect of all the other members of the system. Self-consistent dynamics is ubiquitous in nature. For example, in plasma physics the dynamics of an ensemble of charged particles is determined by the electromagnetic fields generated by the particles themselves. In gravitational systems, the dynamics of an ensemble of masses is determined by the gravitational potential created by all the particles in the system. In hydrodynamics, an ensemble of point vortices evolves under the advection of the velocity field generated by the vortices themselves. Although the equations governing the above mentioned systems have been known for quite a long time (e.g., the Lorentz force and Maxwell's equations in the case of a plasma) their self-consistent dynamics is not well-understood. For example, a lot is known about the chaotic dynamics of a single charged particle in a given, time-dependent electrostatic wave. But, much less is known about the problem of self-consistent chaos in an ensemble of charged particles. One of the main goals of this chapter is to study the problem of self-consistent dynamics and chaos in particular in the context of a simple Hamiltonian mean field model known as the single wave model (SWM).

The SWM has its origins in the study of the beam plasma instability [27–29]. More recently, the model has been derived under more general conditions to describe the weakly nonlinear dynamics of marginally stable Vlasov-Poisson

systems [10,11]. Other derivations and applications of the SWM include Ref. [9], the work in Ref. [1] where the mean field–particle Lagrangian of the model was derived from the full N-body classical mechanics Lagrangian for Coulomb interactions, the study of the model to treat Langmuir turbulence [19], and Landau damping[17,20]. In a more general setting, single wave models have been used to study self-consistent Lagrangian transport [12,13], the relationship between self-consistent chaos and phase space coherent structures [14], finite-amplitude non-axisymmetric perturbation of vortices [4], critical layer dynamics in shear flows [5], and free electron lasers [18].

The organization of this chapter is as follows. In the next section we define the SWM in the finite N and in the $N \to \infty$ limit and discuss the application of the model to fluids and plasmas. Also, in this section we discuss the relationship between the SWM and the Hamiltonian mean field model proposed in Refs. [2,24,6,16]. Section 3 discusses the integrability of the SWM in the finite N case. In particular, using the symmetries and the conservation laws of the model, it is shown that the model is integrable in the $N = 1$ case and in the $N = 2$ symmetric case. These integrable solutions are important because they provide the basic understanding of the coherent structures found in the large N and kinetic limits of the model. Section 4 presents a symplectic map version of the SWM. Section 5 studies the linear theory of the SWM in the kinetic limit. In particular, we derive the dispersion relation and present a criterion that gives necessary and sufficient conditions for the stability of a general equilibrium with a single extremum. In addition, we discuss the initial value problem and Landau damping. Section 6 shows the construction of exact nonlinear solutions of the SWM, which are the analogue of the BGK (Bernstein-Greene-Kruskal) modes in plasma physics [26]. Section 7 is devoted to the study of the role of self-consistent chaos in the formation of coherent structures . Section 8 discusses a self-consistent dynamical bifurcation in the SWM that leads to the destruction of coherent structures and violent mixing of the phase space. The conclusions are presented in Sec. 8, and a derivation of the SWM from the Vlasov-Poisson system is presented in Appendix A.

2 The single wave model

The single wave model (SWM) is a Hamiltonian system consisting of an ensemble of N particles in one-dimension with phase space coordinates (x_j, u_j), $j = 1, 2, \ldots N$, such that

$$\frac{dx_j}{dt} = \frac{\partial H}{\partial u_j}\,, \qquad \frac{du_j}{dt} = -\frac{\partial H}{\partial x_j}\,, \tag{1}$$

where

$$H = \sum_{k=1}^{N} \left[\frac{1}{2}\, u_k^2 - a(t)\, e^{ix_k} - a^*(t)\, e^{-ix_k} \right]\,, \tag{2}$$

$$\frac{da}{dt} - iUa = \frac{i}{N} \sum_{k=1}^{N} \Gamma_k \, e^{-ix_k} \ , \tag{3}$$

and σ, U and Γ_j are parameters.

Equation (2) is the Hamiltonian of an ensemble of particles in the potential of a time-dependent wave with a single harmonic with wave-number $\kappa = 1$. The dynamics of Hamiltonians of this type is well understood in two limits: when $a(t)$ =constant, and when $a(t)$ is a *given* function of time. The first case is fully integrable. In particular, the N particles problem decouples and reduces to the pendulum problem. In the second case, when $a(t)$ is a given function, the system also decouples, but, due to the time dependence, the system is in general not integrable. For example, the case $a = \cos(\omega t)$ leads to the extensively studied periodically perturbed pendulum, which has both integrable and chaotic solutions [25]. The nontrivial aspect of the SWM lays in the fact that the function $a(t)$, rather than being given a priori, is determined by the dynamics itself. That is, according to Eq. (3), the dynamics of the particles, $x_j(t)$, determines the dynamics of the field, $a(t)$. In this respect, the SWM is a *self-consistent* model.

The SWM is a *mean field* model; it treats the interacting elements of the system as independent entities moving in an average field determined self-consistently from the dynamics of all the elements. Defining

$$a = \sqrt{J} \, e^{-i\theta} \, , \tag{4}$$

and writing the SWM as

$$\frac{d^2 x_j}{dt^2} = -\frac{\partial V}{\partial x_j} \, , \qquad V = -2\sqrt{J} \, \cos(x_j - \theta) \, , \tag{5}$$

it is clearly seen that the equations governing the dynamics of the N interacting particles reduce to the equation governing the motion of a single particle under the effective potential V. That is, the only influence a particle has in the rest is through its contribution to the effective potential which is determined from Eq. (3).

In the kinetic limit ($N \to \infty$), the system is described by a phase distribution function f, evolving according to the Vlasov equation

$$\partial_t f + \partial_u H \ \partial_x \, f - \partial_x \, H \, \partial_u \, f \ = 0 \, , \tag{6}$$

with

$$H = \frac{u^2}{2} - a(t) \, e^{i\,x} - a^*(t) \, e^{-i\,x} \, , \tag{7}$$

$$\sigma \frac{da}{dt} - iUa = \frac{i}{2\pi} \int e^{-ix} \, dx \int du \, f \, . \tag{8}$$

The extra parameter σ (which in the finite N case was taken to be $\sigma = 1$) has been introduced for convenience when comparing with the HMF (Hamiltonian mean field model) which corresponds to $\sigma = 0$ [2,16].

Most of the studies of the SWM so far have limited attention to the case $\Gamma_k > 0$. In fact, early derivations of the model in the context of the beam-plasma instability considered compact electron equilibrium distributions for which only positive Γ_k are acceptable [27,28,1]. However, in the description of generic instabilities of marginal stable plasmas it is possible to have positive and negative Γ_k's [10,13]. In this case the starting point is a marginally stable background plasma equilibrium density. Perturbations that locally increase the equilibrium density have $\Gamma_k > 0$ and are called "clumps," while perturbations that locally deplete the equilibrium density have $\Gamma_k < 0$ and are called "holes." In the fluid dynamics context, the interpretation of the Γ_k's is straightforward: Γ_k is the circulation of the point vortex k that can be negative or positive. Consideration of Γ_k's with different signs opens a new chapter in the study of mean field coupled Hamiltonian systems from the physical and the dynamical systems point of view.

The SWM is a universal model describing the dynamics of marginally stable Vlasov-Poisson systems. By universal we mean that the model describes the dynamics of a large class of instabilities, and it does not depend on the details of the long-range interactions involved. In particular the SWM describes the weakly nonlinear dynamics of Vlasov-Poisson system of the form

$$\partial_T F + u\,\partial_X F + \partial_u (F_0 + F)\,\partial_X \Phi = 0\,, \tag{9}$$

$$G(k)\,\tilde{\Phi}(k,T) = -\int_{-\infty}^{\infty} \tilde{F}(k,u,T)du\ , \tag{10}$$

where the tilde denotes Fourier transform. Appendix A presents a derivation of the SWM from Eqs. (9)-(10), further details can be found in Refs. [10,11].

In the plasma physics case, according to Poisson equation,

$$G(k) = k^2\,, \tag{11}$$

and Eq. (9) is the kinetic equation for the electron distribution function in a uniform neutralizing ion background with $F(X,u,T)$ denoting the departure from the equilibrium $F_0(u)$ [26]. Here time and space have been normalized using the electron plasma frequency, $\omega_e^2 = 4\pi n_0 e^2/m$, and the Debye length, $\lambda_D = V/\omega_e$, respectively, where e is the electron charge, m is the electron mass, n_0 is the equilibrium plasma density, and V is a chosen velocity scale. The distribution function, and potential are nondimensionalized with V/n_0 and $e/(mV^2)$ respectively, and thus $\int_{-\infty}^{\infty} F_0\,du = 1$.

However, the validity of the SWM does not depend on the specific functional form of $G(k)$. Another important case is

$$G(k) = 2k\coth(k)\,, \tag{12}$$

which corresponds to the vorticity defect model that describes the dynamics of localized vorticity perturbations in a strong shear flow [3]. In this context, the Vlasov equation plays the role of the vorticity advection equation, with $F + F_0$ representing the vorticity, and the (x,u) phase space coordinates playing the role

of the (x, y) spatial coordinates of a two-dimensional incompressible fluid. The specific form of the function G in this case arises from a matched asymptotic expansion that divides the fluid in two regions; an outer region dominated by a constant vorticity Couette flow and an inner region over which the vorticity varies rapidly. The vorticity defect model provides an interesting link between the SWM model and fluid dynamics, passing through an analogy with the Vlasov-Poisson equation. However, as discussed in Refs. [8,21,4,5] the SWM, and generalizations of it, can be derived directly from the fluid dynamics equations including the two-dimensional Euler equation and the β-plane equation describing quasigeostrophic flows.

The HMF model [2,16]

$$\frac{d^2 x_j}{dt^2} = -\frac{\epsilon}{N} \sum_{k=1}^{N} \sin(x_j - x_k)\,, \tag{13}$$

is a special case of the single wave model when the first term, da/dt, on the left hand side of Eq. (3) vanishes, and

$$U = -\frac{2}{\epsilon}\,, \qquad \Gamma_k = 1\,, \tag{14}$$

where in this case, the mean field a corresponds to the magnetization

$$M = \frac{1}{N} \sum_{k=1}^{N} e^{i x_k} = \frac{2}{\epsilon}\, a\,. \tag{15}$$

In the kinetic description the HMF model is recovered from Eqs. (6)-(8) when $\sigma = 0$. In this special case, the Hamiltonian in Eq. (6) can be rewritten as

$$H = \frac{u^2}{2} + V(x,t)\,, \qquad \partial_x^2 V = \frac{\epsilon}{2\,\pi} \int dx' \int du\, \cos(x - x')\, f(x', u, t)\,, \tag{16}$$

which is the kinetic model in [2], except for a trivial $1/(2\pi)$ normalization factor.

3 Symmetries, conservation laws, and integrability

Defining

$$p_k = \Gamma_k\, u_k\,, \qquad a = \sqrt{\frac{J}{N}}\, e^{-i\theta}\,, \tag{17}$$

the SWM model can be written as the $N + 1$ Hamiltonian system

$$\frac{dx_k}{dt} = \frac{\partial \mathcal{H}}{\partial p_k}\,, \qquad \frac{dp_k}{dt} = -\frac{\partial \mathcal{H}}{\partial x_k}\,, \tag{18}$$

$$\frac{d\theta}{dt} = \frac{\partial \mathcal{H}}{\partial J}\,, \qquad \frac{dJ}{dt} = -\frac{\partial \mathcal{H}}{\partial \theta}\,, \tag{19}$$

where the Hamiltonian

$$\mathcal{H} = \sum_{j=1}^{N} \left[\frac{1}{2\Gamma_j} p_j^2 - 2\Gamma_j \sqrt{\frac{J}{N}} \cos(x_j - \theta) \right] - UJ \ , \tag{20}$$

is a function of the canonical conjugate coordinates of the particles (x_j, p_j), and the canonically conjugate coordinates of the mean field (θ, J). The invariance of Hamiltonian in Eq. (20) under time translations, $t \to t + \tau$, implies the conservation of the energy $\mathcal{E}$, which in (x_j, u_j, a) coordinates can be written as

$$\mathcal{E} = \frac{1}{N} \sum_{j=1}^{N} \Gamma_j \left(\frac{u_j^2}{2} - a\, e^{ix_j} - a^*\, e^{-ix_j} \right) + U\, |a|^2 \, . \tag{21}$$

The Hamiltonian is also invariant under space translations $(x_k, \theta) \longmapsto (x_k + \alpha, \theta + \alpha)$, and this leads to the conservation of the total momentum $\mathcal{P}$

$$\mathcal{P} = \frac{1}{N} \sum_{j=1}^{N} \Gamma_j \ u_j + |a|^2 \, . \tag{22}$$

The first term on the right-hand side of this equation is the momentum of the particles, and the second term is the momentum of the mean field.

Under the time-dependent canonical transformation

$$x_k \to x_k + Ut \, , \qquad p_k \to p_k + \Gamma_k U \, , \tag{23}$$

$$\theta \to \theta + Ut \ , \qquad J \to J \, , \tag{24}$$

the Hamiltonian transforms as $\mathcal{H} \to \mathcal{H} + U\, J$. Therefore, without loss of generality we can assume that $U = 0$. In noncanonical variables, this transformation corresponds to a Galilean transformation $(x_k, u_k) \to (x_k + Ut, u_k + U)$, $a \to a \exp(-iUt)$.

When $U = 0$, the Hamiltonian Eqs. (18)-(19) are invariant with respect to the transformation

$$(x_k, \theta, \Gamma_k) \longmapsto (-x_k, -\theta, -\Gamma_k) \ . \tag{25}$$

In noncanonical coordinates this transformation corresponds to a reflection of the particles with respect to the origin in the (x_j, u_j) space, accompanied by a change in sign in Γ_k, and the complex conjugation of the mean field

$$(x_k, u_k, \Gamma_k, a) \longmapsto (-x_k, -u_k, -\Gamma_k, a^*) \ . \tag{26}$$

Initial conditions invariant under the transformation in Eq. (26) are called *symmetric states*. In general, an N-particles symmetric state consists of $N/2$ clumps (i.e., particles with $\Gamma_k > 0$) symmetrically opposed to $N/2$ holes (i.e., particles with $\Gamma_k < 0$) that is

$$(x_j, u_j) = -(x_{j+N/2}, u_{j+N/2}) \, , \qquad \Gamma_j = -\Gamma_{j+N/2} \, , \qquad a_i = 0 \tag{27}$$

where $j = 1, \dots N/2$, and a_i is the imaginary part of the mean field that vanishes because $a = a^*$. Because the equations are invariant under this transformation, symmetric states remain symmetric for all time, and thus a symmetric state with N particles can be effectively regarded as a system with $N/2$ particles.

In general, a state with N particles is a $N+1$ degrees-of-freedom Hamiltonian system, and according to the Liouville-Arnold theorem, integrability requires $N+1$ constants of motion. The only known constants of motion are the momentum and the energy and thus the $N + 1 = 2$ system consisting of one particle in the mean field is integrable [29]. Because in general there are no other known constants of motion, this seems to be the only fully integrable case of the single wave model. The following subsection discusses this solution. However, when limiting attention to symmetric states the $N = 2$ system is also integrable [14]. In this case, the system has $N/2+1 = 2$ degrees of freedom and, as described in subsection 3.2, use of the momentum conservation law allows the integration of the solution. The main role of SWM is to describe the mean field interaction of systems composed of a large, or even infinite, number of particles. In this regard the integrability of the model in the $N = 1$ and $N = 2$ cases might seem like an academic issue. However, this is not the case. As we will discuss in Sec. 7, these low degree of freedom integrable solutions provide the key elements for the description of coherent states with $N \gg 1$ and $N \to \infty$.

3.1 Integrability of the $N = 1$ model

When there is only one particle, the single wave Hamiltonian has two degrees of freedom, one for the particle and one for the wave. Using the momentum conservation law, the problem can be reduced to one degree of freedom [29]. To do this, we define $q = x - \theta$, substitute the expression for the momentum $\mathcal{P}$ in Eq. (20) with $N = 1$ and get

$$\mathcal{H} = \frac{1}{2\Gamma}\, p^2 - 2\Gamma\sqrt{\mathcal{P} - p}\, \cos q\,. \tag{28}$$

Since this Hamiltonian is time-independent, and it has only one degree of freedom, it is completely integrable. In particular, the particle orbits in the phase space follow the constant energy contours, $\mathcal{H} =$ constant.

The fixed points of the Hamiltonian (28), defined by the condition

$$\dot{q} = \frac{\partial H}{\partial p} = 0\,, \qquad \dot{p} = -\frac{\partial H}{\partial q} = 0\,, \tag{29}$$

are determined by the solutions of

$$\sin q = 0\,, \qquad p\sqrt{\mathcal{P} - p} + \Gamma^2\, \cos q = 0\ . \tag{30}$$

The first equation has two solutions $q = 0$ and $q = \pi$. In the first case there is only one solution of the second equation in (30) for p. In the second case, when $q = \pi$, there are no solutions for p, except when

$$\frac{3}{4^{1/3}} < \frac{\mathcal{P}}{\Gamma^{4/3}}\,, \tag{31}$$

in which case there are two solutions for p. Thus, as shown in Fig. 1, there is a fixed point at $(0, p_0)$ with $p_0 < 0$; and, if condition (31) is satisfied, there are two other fixed points at (π, p_1), and (π, p_2).

The stability of the fixed points is determined by linearizing the equations of motion. Doing this, we conclude that (π, p_1) is stable and (π, p_2) unstable. The fixed point at $(0, p_1)$ is stable, and it corresponds to a particle oscillating at the bottom of the potential with oscillation frequency

$$\omega^2 = 2\sqrt{\mathcal{P} - p_0}\left[1 + \frac{\Gamma^2}{2\left(\mathcal{P} - p_0\right)^{3/2}}\right] . \tag{32}$$

3.2 Integrability of $N = 2$ symmetric states

To construct symmetric integrable solutions, consider an $N = 2$ state consisting of one clump and one hole with $\Gamma_1 = -\Gamma_2 = \Gamma$, $U = 0$, and symmetric initial conditions $x_1(0) = -x_2(0)$, $u_1(0) = -u_2(0)$, and $a(0) = a^*(0)$. Substituting $x_1(t) = -x_2(t) = x(t)$, $u_1(t) = -u_2(t) = u(t)$ and $a(t) = a^*(t)$ into Eqs. (1)–(3), we get

$$\frac{dx}{dt} = u\,, \qquad \frac{du}{dt} = -2\,a\sin x\ , \qquad \frac{da}{dt} = \Gamma\sin x\,. \tag{33}$$

This system of three ordinary differential equations can be reduced to a two-dimensional integrable system using the conservation of momentum

$$\mathcal{P} = \Gamma u + a^2\,. \tag{34}$$

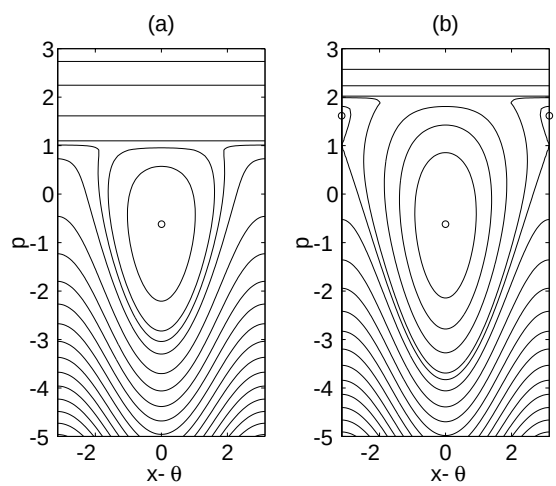

Fig. 1. Phase space of reduced, $N = 1$, single wave model Hamiltonian in Eq. (28). Panel (a) shows the case $\Gamma = 1$, $\mathcal{P} = 1$, and panel (b) shows the case $\Gamma = 1$, $\mathcal{P} = 2$. In both cases, the stable fixed point at $x - \theta = 0$ corresponds to the particle at the bottom of the single-wave potential. Consistent with Eq.(31), in case (b) there is a stable and an unstable fixed point at $x - \theta = \pi$.

In this case, the conservation of energy is of no use because for symmetric states the energy vanishes identically, $\mathcal{E} = 0$.

For the two-dimensional reduction, we take x and a as basic variables. Solving for u in Eq. (34) and substituting the result in (33), we conclude that the dynamics of the (x, a) variables is governed by the Hamiltonian system

$$\frac{dx}{d\tau} = \frac{\partial H}{\partial A}\,, \qquad \frac{dA}{d\tau} = -\frac{\partial H}{\partial x}\,, \tag{35}$$

with Hamiltonian

$$H = \alpha\, A - \frac{A^3}{3} + \cos x\,, \tag{36}$$

where we have introduced the rescaled variables

$$A = a\Gamma^{-2/3}\,, \qquad \tau = \Gamma^{1/3}\, t\,, \qquad \alpha = \mathcal{P}\Gamma^{-4/3}\,. \tag{37}$$

Once A and x are found, u is determined from

$$u = \frac{\mathcal{P}}{\Gamma}\left(1 - \frac{A^2}{\alpha}\right)\,. \tag{38}$$

Since the Hamiltonian (36) is time independent, the system is completely integrable and the orbits follow the contours H =constant.

As shown in Fig. 2, when $\alpha < 0$, the system (35) has no fixed points, and when $\alpha > 0$ the system has four fixed points: $(x_0, A_0) = (0, \sqrt{\alpha})$, $(0, -\sqrt{\alpha})$, $(\pi, \sqrt{\alpha})$, and $(\pi, -\sqrt{\alpha})$, with eigenvalues $\lambda = \pm i\omega_0$, $\lambda = \pm\omega_0$, $\lambda = \pm\omega_0$, and $\lambda = \pm i\omega_0$, respectively, where

$$\omega_0 = \sqrt{2}\alpha^{1/4}. \tag{39}$$

That is the elliptic and hyperbolic fixed points come in pairs since the equations of motion Eq. (35) are invariant under the transformation $(x, a) \longmapsto (x+\pi, -a)$. The value $\alpha = 0$ is the bifurcation point at which an elliptic-hyperbolic pair is created at $x = 0$, and another elliptic-hyperbolic pair is created at $x = \pm\pi$. A perturbative solution of the equations of motion of the Hamiltonian (36) gives a a nonlinear correction to the rotation frequency

$$\omega = \left[1 - \left(\frac{5 + 9\lambda}{12}\right)\varepsilon^2\right]\omega_0\,, \qquad \lambda = \left(\frac{\alpha}{\alpha_*}\right)^{3/2}\,, \tag{40}$$

and

$$A(\tau) = \frac{\omega_0^2}{2}\left[1 - 2\,\varepsilon\,\cos\omega\,\tau - \varepsilon^2\left(1 - \frac{2}{3}\,\cos\omega\tau - \frac{1}{3}\,\cos 2\,\omega\,\tau\right)\right]\,, \tag{41}$$

$$x(\tau) = \omega_0^3\left[\varepsilon\,\sin\omega\,\tau - \frac{\varepsilon^2}{3}\,(\sin\omega\,\tau + \sin 2\,\omega\,\tau)\right]\,, \tag{42}$$

where

$$\varepsilon = \frac{\sqrt{\alpha} - A(0)}{\omega_0^2} \ll 1\,, \tag{43}$$

is a small parameter measuring the departure of the initial condition $(x(0), A(0))$ from the $(\sqrt{\alpha}, 0)$ elliptic fixed point. The interested reader should refer to [14] for the details of the calculation.

As observed in Fig. 2, for different values of α, the phase space topology of the H =constant contours change. These global bifurcations are caused by separatrix reconnection. In a Hamiltonian system a separatrix is a distinguished orbit that joins the unstable and stable manifolds of hyperbolic points. Separatrix reconnection corresponds to the different ways in which the hyperbolic points can connect. In panel (b) of Fig. 2 the separatrices join the unstable and stable manifolds of the same point, whereas in panel (c) the separatrices reconnect and join different hyperbolic points. The reconnection threshold can be obtained from the condition $H(P_0) = H(P_\pi)$, where $P_0 = (0, -\sqrt{\alpha})$, and $P_\pi = (\pi, \sqrt{\alpha})$. This condition gives $\alpha_* = (3/2)^{2/3}$. For $\alpha < \alpha_*$, the H =constant contours have the homoclinic topology of Fig. 2-(b), and for $\alpha > \alpha_*$ the heteroclinic topology of Fig. 2-(c). Using (37) the separatrix reconnection bifurcation can be parametrized in terms of the momentum of the system according to

$$\mathcal{P} < \left(\frac{3\,\Gamma^2}{2}\right)^{2/3} \quad \text{Homoclinic}\,, \qquad \mathcal{P} > \left(\frac{3\,\Gamma^2}{2}\right)^{2/3} \quad \text{Heteroclinic}\,, \tag{44}$$

with $\mathcal{P} = (3\,\Gamma^2/2)^{2/3}$ giving the reconnection threshold. Further discussion on separatrix reconnection can be found in Ref. [15].

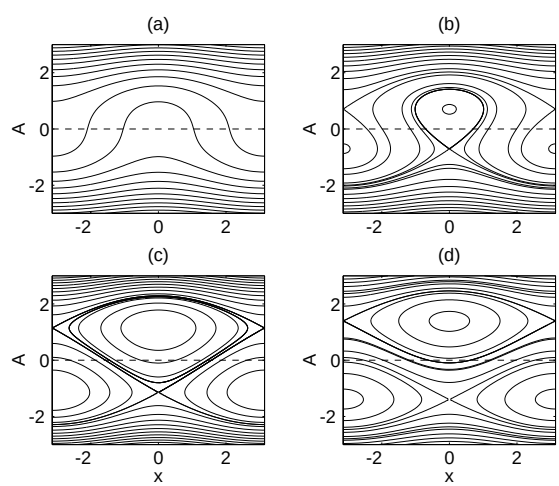

Fig. 2. Phase space of reduced, $N = 2$, single wave model Hamiltonian in Eq. (36). Panel (a) $\alpha = -0.2$, (b) $\alpha = 0.5$, (c) $\alpha = (3/2)^{2/3}$, and (d) $\alpha = 1.95$. In (a) there are no fixed points, case (c) corresponds to the separatrix reconnection threshold, case (b) shows the homoclinic topology, and case (d) the heteroclinic topology.

4 Symplectic map formulation

Symplectic maps arise naturally in the study of Hamiltonian systems. A well-known example is the standard map which is an area preserving transformation of the (q, p) plane defined as

$$\begin{aligned} q^{n+1} &= q^n + p^{n+1} \\ p^{n+1} &= p^n - \kappa \sin q^n \ , \end{aligned} \tag{45}$$

where (q^n, p^n) are phase space coordinates at the discrete time n, and κ is a parameter. The main advantage of maps rests in their relative mathematically simplicity, compared with the time-continuous Hamiltonian systems. Whereas continuous dynamical systems can be time-consuming to integrate numerically, especially for very long times and many initial conditions, maps are very efficient. Another advantage is that maps are relatively simpler to study analytically than their continuous analogues. Because of this, maps are useful to carry out numerical studies of asymptotic properties of Hamiltonian systems.

In this section we discuss a map that is the discrete version of the single wave model. Given a set of differential equations, a map can be obtained by discretizing the time derivatives. However, in the case of Hamiltonian systems, special care must be taken to preserve the symplectic nature of the dynamics. For example, the standard map can be obtained from the time-discretization of the equations of motion of a pendulum, but whereas the map in Eq. (45) is an area preserving transformation, other discretization might not be. One way of to guarantee that a map will be symplectic is to define it using a generating function. Let $(\mathbf{q}^n, \mathbf{p}^n)$ denote the canonical conjugate coordinates of an M-dimensional Hamiltonian system at time n. Then, the transformation $(\mathbf{q}^n, \mathbf{p}^n) \to (\mathbf{q}^{n+1}, \mathbf{p}^{n+1})$ defined by

$$\mathbf{q}^{n+1} = \frac{\partial S}{\partial \mathbf{p}^{n+1}} \, , \qquad \mathbf{p}^n = \frac{\partial S}{\partial \mathbf{q}^n} \tag{46}$$

defines a symplectic map with generating function $S = S(\mathbf{q}^n, \mathbf{p}^{n+1})$. Equation (46) defines a canonical transformation, consistent with the fact the evolution of a Hamiltonian system is a canonical transformation.

Let $\mathbf{q}^n = (x_1^n, x_2^n, \ldots x_N^n, \theta)$ and $\mathbf{p}^n = (p_1^n, p_2^n, \ldots p_N^n, J)$ denote the canonical conjugate coordinates of the single wave model Hamiltonian at time n, and define

$$S = \sum_{j=1}^{N} \left[x_j^n \, p_j^{n+1} + \frac{\tau}{2\,\Gamma_j} \left(p_j^{n+1}\right)^2 - 2\,\tau \sqrt{J^{n+1}}\, \Gamma_j \, \cos\left(x_j^n - \theta\right) \right] + \theta^n \, J^{n+1} \, . \tag{47}$$

Substituting this generating function into Eq. (46) we get the symplectic map

$$X_k^{n+1} = X_k^n + \left(\frac{\tau}{\Gamma_k}\right) p_k^{n+1} \tag{48}$$

$$p_k^{n+1} \ = p_k^n - 2\tau \Gamma_k \sqrt{J^{n+1}} \, \sin(X_k^n - \Theta^n) \tag{49}$$

$$\Theta^{n+1} = \Theta^n - \frac{\tau}{\sqrt{J^{n+1}}} \sum_{j=1}^{N} \Gamma_j \cos(X_j^n - \Theta^n) \tag{50}$$

$$J^{n+1} = J^n + 2\tau\sqrt{J^{n+1}} \sum_{j=1}^{N} \Gamma_j \sin(X_j^n - \Theta^n) \ , \tag{51}$$

for $k = 1, 2, \ldots N$. As expected, this map is a symplectic, time-discretization of the single wave model equations of motion defined in Eqs. (18)-(20), where without loss of generality we have assumed that $U = 0$.

The momentum of the system at time n is

$$\mathcal{P}^n = \sum_{j=1}^{N} p_j^n + J^n \ , \tag{52}$$

and the conservation of momentum in the SMW implies the conservation of the momentum in the map

$$\mathcal{P}^{n+1} = \mathcal{P}^n \, . \tag{53}$$

On the other hand, whereas the continuous model conserves the energy $\mathcal{E}$, in the map the energy is only conserved to first order in the map parameter τ. In general, energy conservation is problematic with maps because of the time discretization.

To simplify the notation we define:

$$x_k^n = X_k^n \ \ , y_k^n = \left(\tfrac{\tau}{\Gamma_k}\right) p_k^n \ \ , \theta^n = \Theta \ \ , \kappa^n = 2\tau^2 \sqrt{J^n} \ , \tag{54}$$

$$\gamma_k = 2\tau^3 \Gamma_k \, , \qquad \Omega = U\tau \, , \qquad \eta^n = \sum_{j=1}^{N} \gamma_j \sin\left(x_j^n - \theta^n\right) \ , \tag{55}$$

and write the SWM map as

$$x_k^{n+1} = x_k^n + y_k^{n+1} \ , \tag{56}$$

$$y_k^{n+1} = y_k^n - \kappa^{n+1} \sin\left(x_k^n - \theta^n\right) \ , \tag{57}$$

$$\kappa^{n+1} = \sqrt{\left(\kappa^n\right)^2 + \left(\eta^n\right)^2} + \eta^n \ , \tag{58}$$

$$\theta^{n+1} = \theta^n - \Omega + \frac{1}{\kappa^{n+1}} \frac{\partial \eta^n}{\partial \theta^n} \ . \tag{59}$$

Note that in doing this we have gone from the implicit J^n map in (51) to the explicitly κ^n map in (59). Comparing Eq. (45) with Eqs. (56)-(59) one observes that the SWM map has the structure of an ensemble of standard maps coupled through a mean field with amplitude κ^n and phase θ. Whereas in the standard map, the parameter κ is fixed, in the SWM map this parameter is self-consistently coupled to the dynamics of the particles [13].

5 Kinetic linear theory: stability and Landau damping

In this section we return to the kinetic description of the single wave model. An important problem in kinetic theory is the stability of solutions. The simplest problem is the linear stability of solutions of the form $f = f_0(u)$, $a = 0$. To study this problem we substitute

$$f = f_0(u) + \sum_{n=-\infty}^{\infty} \psi_n(u,t)\, e^{inx} \,, \qquad a = a_1(t) \tag{60}$$

into Eqs. (6)-(8), neglect the nonlinear terms, and get the linear stability equations

$$\partial_t \psi_n + inu\, \psi_n + i\delta_{n,\pm 1}\, f_0'\, a_1 = 0 \ , \tag{61}$$

$$\sigma \frac{da_1}{dt} - iUa_1 = i \int_{-\infty}^{\infty} \psi_1(u,t) du \ . \tag{62}$$

Assuming a normal mode solution,

$$\psi_n(u,t) = \xi_n(u)\, e^{-ict} \qquad a_1(t) = \rho\, e^{-ict} \ , \tag{63}$$

we get from (61) the eigenfunctions

$$\xi_n(u) = -\frac{\rho f_0'}{u-c}\, \delta_{n,\pm 1} \ , \tag{64}$$

and the *dispersion relation*

$$D(c) \equiv \sigma c + U - \int_{-\infty}^{\infty} \frac{f_0'}{u-c}\, du = 0 \ , \tag{65}$$

where $c = c_r + ic_i$.

An equilibrium solution $f = f_0(u)$, $a = 0$ is linearly stable with respect to normal mode perturbations if and only if there are no solutions of Eq. (65) with $c_i > 0$. As an illustrative example, a normalized Lorentzian equilibrium with "temperature" $T = 1/\beta$

$$f_0 = \frac{\sqrt{\beta}}{\pi} \frac{1}{1+\beta\, u^2} \,. \tag{66}$$

In this case the integral can be calculated using the Cauchy residue theorem, and it is concluded that the equilibrium is unstable if and only if $\epsilon > 2/\beta$, in which case

$$c = \pm i \left(\sqrt{\frac{\epsilon}{2}} - \frac{1}{\sqrt{\beta}} \right) \,. \tag{67}$$

In the previous examples, the integral of the dispersion relation was easy to compute. However, in general this is not the case, and it is important to derive general stability criteria to determine the stability of equilibria without the need of explicitly solving the dispersion relation. In Ref. [11] the Nyquist method was used to derive stability criteria for general equilibria. Here we quote the result

for the case of equilibria with a single extremum; the interested reader can find further details in Ref. [11]. An equilibrium f_0 with a single maximum at $u = u_1$ is unstable if and only if

$$u_1 + U + \int_{-\infty}^{\infty} \frac{f_0(u_1) - f_0(u)}{(u_1 - u)^2} du > 0 \ . \tag{68}$$

If the extremum is a minimum the inequality sign is reversed. In the HMF model case, Eq. (16), an equilibrium $f_0(u)$ with a single maximum at $u = 0$ is unstable if and only if

$$2 < \epsilon \int_{-\infty}^{\infty} \frac{f_0(0) - f_0(u)}{u^2} \, du \, . \tag{69}$$

As a particular example, consider a Gaussian distribution with temperature $T = 1/\beta$

$$f_0(u) = \sqrt{\frac{\beta}{2\pi}} \exp\left(-\beta \frac{u^2}{2}\right) \ . \tag{70}$$

In this case we have that the equilibrium is unstable if and only if

$$\epsilon > \frac{2}{\beta} \, . \tag{71}$$

That is, decreasing the temperature or increasing the coupling leads to instability.

5.1 High frequency oscillations

In a way similar to what is done in a Vlasov-Poisson plasma, one can look for pure real solutions of the dispersion relation for a general distribution $f_0(u)$ with temperature $T =< u^2 >$ in the limit

$$T \ll c^2 \, . \tag{72}$$

This is the analogue of the Langmuir waves in plasma physics. In this case, assuming $f_0(u) = 0$ for $|u| > u_*$, the integral in the dispersion relation can be expanded as

$$\int_{-\infty}^{\infty} \frac{f_0'}{u - c} \, du \approx \int_{-u_*}^{u_*} \frac{f_0}{(u - c)^2} \, du \approx \frac{1}{c^2} \int_{-u_*}^{u_*} f_0 \left(1 + \frac{2u}{c} + \frac{3u^2}{c^2} \ldots\right) du \, , \tag{73}$$

doing the integrals

$$\sigma c^3 + U c^2 - 1 - 3(T/c^2) = 0 \, . \tag{74}$$

In the SWM case, $\sigma = 1$, $U = 0$, we can solve this equation by a perturbation expansion in T/c^2 to get

$$c = (3T + 1)^{1/3} \, . \tag{75}$$

In the $\sigma = 0$, HMF model case, Eq. (16), a perturbative solution of the dispersion relation gives

$$c = 3T - \epsilon/2 \, , \tag{76}$$

which generalizes the result reported in [2] for the case of a "water-bag" equilibrium distribution. Equations (75) and (76) are the analogue of the Langmuir waves dispersion relation.

5.2 Initial value problem and Landau damping

When $n \neq \pm 1$ the solution of (61) with initial condition $\psi_n(u, t = 0) = \psi_n(u, 0)$, $a_1(t = 0) = a(0)$, is $\psi_n(u, t) = \psi_n(u, 0) \exp(-inut)$, and $f(x, u, t)$ simply phase mixes. The general solution for $n = \pm 1$ is slightly more complicated but it can be obtained in the same way as it is done for the Vlasov-Poisson equation by introducing the Laplace transforms

$$\hat{\psi}(u, p) = \int_0^\infty \psi(u, t) e^{-pt} dt \ , \qquad \hat{a}(p) = \int_0^\infty a(t) e^{-pt} dt \ , \tag{77}$$

where $p = p_r + ip_i$. The convergence of the integrals in (77) requires $p_r \geq p_0$, where p_0 is a real number.

Substituting (77) into (61) and solving for $\hat{a}$, we get

$$\hat{a}(p) = \frac{N(p)}{D(p)} \ , \tag{78}$$

where

$$N(p) = i\sigma a(0) + i \int_{-\infty}^{\infty} \frac{\psi(u, 0)}{u - ip} du \ , \qquad D(p) = i\sigma p + U - \int_{-\infty}^{\infty} \frac{f_0'(u)}{u - ip} du \tag{79}$$

Knowing $N(p)$ and $D(p)$, the mean field a is obtained by inverting the Laplace transform

$$a(t) = \frac{1}{2\pi i} \int_{p_0 - i\infty}^{p_0 + i\infty} \frac{N(p)}{D(p)} e^{pt} dp \ , \tag{80}$$

where the integration is along the Bromwich contour, which is a straight line parallel to the imaginary axis in the complex p-plane and located to the right of the abscissa of convergence. The evaluation of the integral in (80) is simplified by deforming the contour to the left-half of the complex p plane and using the Cauchy residue theorem. However, doing this requires the analytic continuation of the functions $D(p)$ and $N(p)$, originally defined for $p \geq p_0$, into the entire complex plane. One way of performing this analytic continuation is following the Landau prescription according to which the integrals in D and N should be viewed as integral in the complex u-plane and evaluated along a contour that should always pass below the singularity $u = ip$ regardless of the sign of p_r. As in the case of the Vlasov-Poisson system, this prescription allows the determination of the asymptotic value of the integral in (80) and leads to the conclusion that for stable equilibria, $f_0(u)$, the mean field exhibits decay known as Landau damping [23,26]. However, as in the plasma and fluid dynamics cases, one should be aware of technical difficulties that can lead to more general time asymptotic behavior [30,3]. Here we limit attention to an analytical tractable example that illustrates Landau damping in the context of the HMF model.

The equilibrium considered is the normalized Lorentzian distribution in Eq. (66). In this case, the integral in (79) can be easily computed and analytically continued giving:

$$\mathcal{D}(p) = -\frac{2\,\beta}{\epsilon} \frac{(p - p_+)(p - p_-)}{(\sqrt{\beta}\, p + 1)^2} \ , \qquad p_\pm = \pm\sqrt{\frac{\epsilon}{2}} - \frac{1}{\sqrt{\beta}} \ . \tag{81}$$

For a perturbation of the form

$$\psi_1(u,0) = \frac{1}{1+\Delta\, u^2}\,, \tag{82}$$

a similar calculation leads to

$$\mathcal{N}(p) = -\frac{\pi}{1+\sqrt{\Delta}\, p}\,. \tag{83}$$

Substituting (81) and (83) into (80) we get

$$a(t) = -\frac{i\,\epsilon}{4\,\beta}\int_{p_0-i\,\infty}^{p_0+i\,\infty} \frac{(\sqrt{\beta}\,p+1)^2\, e^{pt}}{(1+\sqrt{\Delta}\,p)(p-p_+)(p-p_-)}\, dp\,, \tag{84}$$

which can easily be evaluated using the Cauchy residue theorem giving, for $\beta = \Delta$,

$$a(t) = \frac{\epsilon\,\pi}{4\,\sqrt{\beta}}\,\left(e^{p_+ t} - e^{p_- t}\right)\,. \tag{85}$$

Figure3 shows $a(t)$ in (85) for $\epsilon = 2$ and $\beta = 0.5$, 1 and 1.3. According to (67) the Lorentzian equilibrium (66) is unstable if and only if $\epsilon > 2/\beta$. Thus, as expected, case $\beta = 1.3$ in Fig. 3 exhibits a transient followed by an exponential growth due to the linear instability. For $\beta = 0.5$ the equilibrium is stable, and following a transient growth, the mean field Landau damps. The case $\beta = 1$ is the marginal value and gives rise to a neutral oscillation of the mean field.

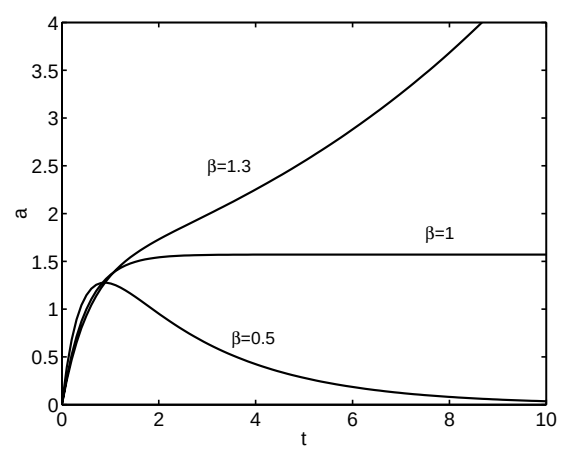

Fig. 3. Instability and Landau damping in the HMF model limit of the SWM model for the Lorentzian equilibrium in Eq. (66) and Lorentzian perturbation of the form in Eq. (82) with $\epsilon = 2$ and $\Delta = \beta$. The critical value of β in this case is $\beta = 1$. For $\beta > 1$ the equilibrium is linearly unstable. For $\beta < 1$ the equilibrium is stable, and the perturbation exhibits Landau damping.

6 Kinetic nonlinear solutions

The kinetic limit of the SWM, Eqs. (6)-(8), admits a large class of exact nonlinear solutions, which are the analogue of the BGK modes for the Vlasov-Poisson system [10,11]. To construct these solutions, we substitute

$$f = f(\xi, u), \qquad a = \rho\, e^{i\delta - ict} \ , \tag{86}$$

into Eqs. (6)-(8), where $\xi = x - c\,t$ and get

$$\frac{\partial(H, f)}{\partial(\xi, u)} = 0 \tag{87}$$

$$\int_{-\infty}^{\infty} du \int_0^{2\pi} d\xi\, f(H)\, e^{-i\xi} = -2\pi(U + \sigma c)\, \rho \ ; \tag{88}$$

where

$$H = \frac{1}{2}(u - c)^2 - 2\rho \cos\xi \ . \tag{89}$$

Any function of the form $f = f(H)$ is a solution of Eq. (87). However, $f = f(H)$ will be a self-consistent solution of (8), only if Eq. (88) is also satisfied. As an example, consider the normalized Gibbs distribution

$$f(H) = \frac{e^{-\beta H}}{\lambda} \ , \tag{90}$$

where $\lambda = \langle e^{-\beta H} \rangle$ is a normalization factor. In this case the self-consistent condition leads to

$$\rho(U + \sigma c) = -\frac{I_1(2\beta\,\rho)}{I_0(2\beta\,\rho)} \ , \tag{91}$$

where $I_1(z)$ is the modified Bessel function of order one [10,11]. In the $\sigma = 0$, HMF model case, Eq. (16), the solution (91) reduces to the one reported in [24].

$$M = \frac{I_1(\epsilon\beta M)}{I_0(\epsilon\beta M)} \ , \tag{92}$$

where M is the magnitude of the magnetization.

7 Self-consistent chaos and coherent structures

The spontaneous formation of coherent structures is commonly observed in experiments and numerical simulations in hydrodynamics and plasmas. Coherent structures are also routinely observed in planetary flows (e.g., the Jupiter's red spot.) These structures typically coexist with a turbulent background, and a problem of interest is to explain their robustness with respect to the chaotic transport induced by the background. The goal of this section is to study this problem in the context of the SWM.

The existence of phase space coherent structures in large degrees-of-freedom Hamiltonian systems is in principle puzzling because coherence requires some degree of integrability, which one might expect to lose as the number of degrees of freedom increases. However, as we will discuss in this section, there are situations in which mean field self-consistent systems exhibit an effective reduction of the number of degrees of freedom, which leads to coherent behavior.

As in the finite N case, the dependence on U in the kinetic description can be removed by a Galilean transformation, and when $U = 0$ the system is invariant under the transformation

$$(x, u, f, a) \longmapsto (-x, -u, -f, a^*) \ . \tag{93}$$

In the kinetic limit, a symmetric state is defined by the condition

$$f(x, u, t) = -f(-x, -u, t) \, , \qquad a(t) = a^*(t) \, , \tag{94}$$

Figure 4 shows an example of a rotating dipolar coherent structure. This

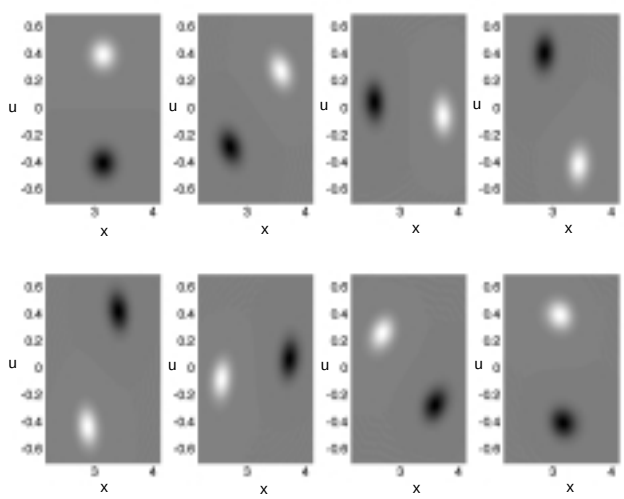

Fig. 4. Rotating dipole obtained from the numerical integration of the kinetic single wave model Eqs. (6)–(7) with initial condition in Eqs. (95)–(96). White corresponds to $f > 0$ (clump), and black to $f < 0$ (hole). The panels show the dipole at $t = 0, \Delta, 2\Delta, \ldots 7\Delta$, where $\Delta = 1.237$ and $7\Delta = 8.66$ is the rotation period of the dipole [14].

state was obtained by integrating numerically the SWM in the kinetic limit, Eqs. (6)-(8), with a symmetric initial condition consisting of a Gaussian distributed hole-clump pair:

$$f(x, u, t = 0) = f_1 - f_2 \, , \qquad a(t = 0) = a_0 \, , \tag{95}$$

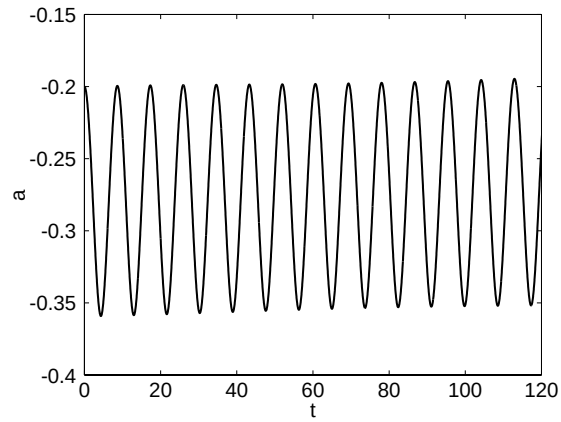

Fig. 5. Real part of mean field a as function of time corresponding to the coherent rotating dipole solution shown in Fig. 4. The imaginary part of a vanishes identically for all t in this case [14].

where

$$f_j = \gamma \exp\left[-\left(\frac{x-x_j}{\sigma_x}\right)^2 - \left(\frac{u-u_j}{\sigma_u}\right)^2\right], \tag{96}$$

$\gamma = 5$, $x_1 = x_2 = \pi$, $u_1 = -u_2 = 0.4$, $a_0 = -0.2$, $\sigma_x = 0.2$, $\sigma_u = 0.1$, and $U = 0$. As the figure illustrates, the structure rotates maintaining its coherence. Figure 5 shows the evolution of the real part of the mean field $a(t)$. Because this is a symmetric state, the imaginary part of a is identically zero. Figure 6 offers a three-dimensional perspective of the hole-clump pair together with a contour plot of the mean field Hamiltonian

$$H = \frac{u^2}{2} - a(t)e^{ix} - a^*(t)e^{-ix}, \tag{97}$$

at a fixed time. As the figure shows, the dipole is trapped in the mean-field potential and rotates around the stable fixed point $(x, u) = (\pi, 0)$. As expected by self-consistency, the rotation period of the dipole is close to the period of the mean field.

Kinetic simulations always introduce some sort of dissipation due to the coarse graining of filamentary structures with a scale beyond the resolution of the numerical method. Because of this, the relationship between very large N discrete particle simulations, which are in principle conservative, and kinetic results might not always be trivial. To explore this issue in the dipole problem, we integrated the finite N SWM model with an initial condition consisting of a discretization of f in Eqs. (95)-(96) with $N = 1000$ (half holes and half clumps) and the appropriate values of Γ_k. In this case, there is not any significant difference between the finite N and the kinetic phase space evolution. However, in the finite N case, the rotation period of the mean field is slightly smaller [14].

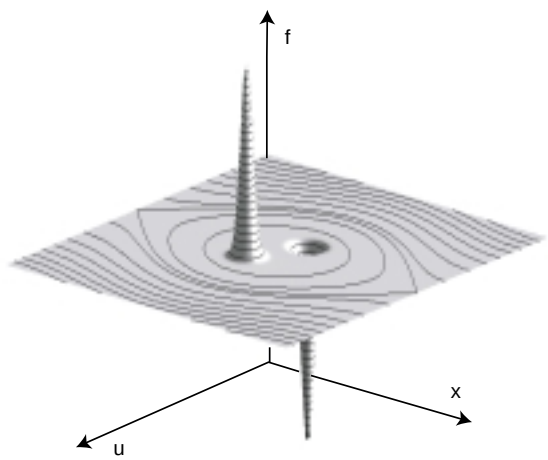

Fig. 6. Three dimensional perspective of a hole-clump dipole in the single wave model. The dipole is trapped in the mean-field potential and rotates around the stable fixed point $(x, u) = (\pi, 0)$ of the mean-field Hamiltonian.

7.1 Macroparticle description

The coherence of the dipole suggests the description of the system as two "macroparticles," one representing the hole and another the clump. The macroparticle representation is a sort of renormalization process in which a group of particles with different values of Γ_k are replaced by one with an effective Γ. For the kinetic initial condition in Eqs. (95)-(96) the effective Γ for the clump is simply

$$\Gamma = \frac{1}{\pi} \int\int f_1 \; dxdu = \gamma \, \sigma_x \sigma_u \, , \tag{98}$$

and for the hole is $-\Gamma$. The macroparticle representation provides a link between systems with large (or infinite) N, and systems with small N, say $N = 1$, or 2. In particular, according to the results discussed in Sec. 3.2, the rotation period of a symmetric hole-clump system is $T = \sqrt{2}\pi/\mathcal{P}^{1/4}$ where $\mathcal{P}$ is the momentum of the $N = 2$ system. The momentum of the kinetic initial condition in Eqs. (95)-(96) is

$$\mathcal{P} = \frac{1}{2\,\pi} \int\int f \, u \; dxdu \; + |a|^2 = \gamma \, u_1 \sigma_x \sigma_u + |a_0|^2 \, , \tag{99}$$

which, according to the macroparticle description, gives the following expression for the rotation period of the kinetic dipole

$$T = \frac{\sqrt{2}\,\pi}{\mathcal{P}^{1/4}} = \frac{\sqrt{2}\,\pi}{\left(\gamma\, u_1 \sigma_x \sigma_u + |a_0|^2\right)^{1/4}} \,. \tag{100}$$

For the parameter values used in Fig. 4, Eq. (100) gives $T = 8.35$ close to the period $T = 8.66$ according to Fig. 5. Equation (40) provides a second order correction of the kinetic dipole rotation period in Eq. (100). To compute this correction note that for the initial condition in Eqs. (95)–(96)

$$\lambda = \frac{2}{3\gamma^2 \sigma_x^2 \sigma_u^2}\, \left(\gamma u_1 \sigma_x \sigma_u + |a_0|\right)^{3/2} \,, \tag{101}$$

which for the parameter values used in Fig. 4, gives $\lambda = 1.5084$. In the evaluation of ε in Eq. (43) we have to take the negative sign of $\sqrt{\alpha}$ because $a(0) = -0.2 < 0$. Doing this, we get $\varepsilon = 0.146$ and $\omega = 1.566$, which gives $T = 8.64$; a value remarkably close to the period $T = 8.66$ according to the numerical results in Fig. 5. Using Eqs. (98), the value of $\alpha = \mathcal{P}\Gamma^{-4/3}$ can be computed, and the topology of the reduced nontwist Hamiltonian of the macroparticles determined. In particular, for the kinetic simulation in Fig. 4, $\alpha = 1.7235 > \alpha_*$, which corresponds to the heteroclinic topology.

A rotating dipole creates a time periodic self-consistent mean field. In dynamical systems, it is well known that time periodic Hamiltonian systems typically give rise to chaos[1] and an important problem is to understand the effect of chaos in the dipole. To this end, consider the evolution of "test" particles with phase space coordinates $(q, \dot{q})$ in the mean field of the rotating dipole

$$\frac{d^2 q}{d\tau^2} = 2A(\tau)\, \sin q \,, \tag{102}$$

where A is give by Eq. (41).

Panel (a) of Fig. 7 shows a snapshot of the rotating dipole at time τ_0, and panel (b) shows a Poincare section of the system in Eq. (102) with $A(\tau_0 + T) = A(\tau_0)$ where T is the fundamental period of the self-consistent mean field. As it is usually the case in Hamiltonian systems, the perturbation gives rise to chaos in the separatrix region. However, in this region the distribution function f is negligible and so is the effect of chaos. On the other hand the perturbation creates islands of stability that "shield" the hole and the clump from the chaotic region. As the dipole rotates, the phase of the Poincare section changes and the islands of integrability follow the motion of the coherent structure.

7.2 Parametric resonance

The frequency of the self-consistent mean field is close to the rotation frequency of the dipole, and there is the possibility of parametric resonance. To explore

[1] We say typically because there are special cases in which the time dependence in the Hamiltonian can be eliminated with an appropriate time-dependent canonical transformation.

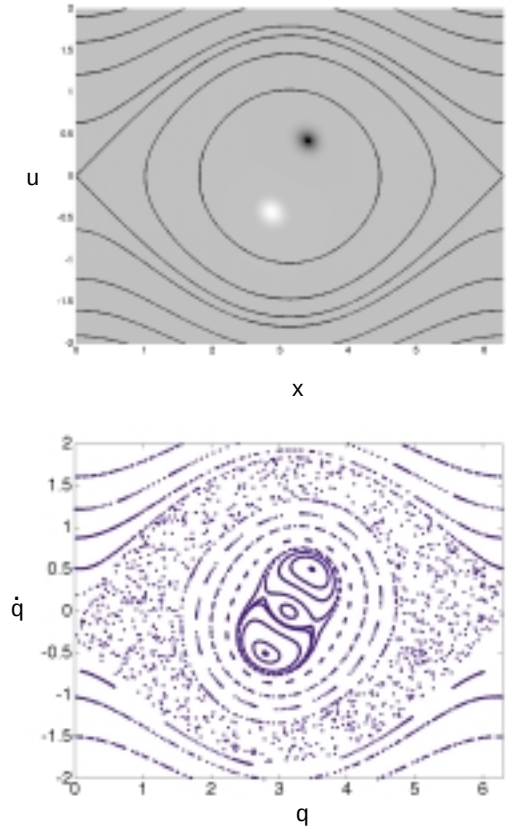

Fig. 7. The top panel show contour plots of the rotating dipole solution at a fixed time along with the contour lines of the Hamiltonian in Eq. (2). The panel on the bottom shows a Poincare section in the mean field of the rotating dipole solution.

the effect of this resonance in the coherence of the dipole, consider a symmetric state with N particles, $N/2$ holes, and $N/2$ clumps, and define the center of mass coordinates

$$\bar{x} = \frac{2}{N} \sum_{j=1}^{N/2} \Gamma_j \, x_j \, , \qquad \bar{u} = \frac{2}{N} \sum_{j=1}^{N/2} \Gamma_j \, u_j \, . \tag{103}$$

Substituting Eq. (103) into Eq. (1), and assuming $x_j \ll 1$ we have

$$\frac{d\bar{x}}{dt} = \bar{u} \, , \qquad \frac{d\bar{u}}{dt} = -2 \, a \sin \bar{x} \ , \qquad \frac{da}{dt} = \sin \bar{x} \, . \tag{104}$$

Comparing with Eq. (33), it is concluded that, in this approximation, the evolution of the center of mass of the hole-clump dipole is described by the integrable

$N = 2$ system. Let

$$q_j = x_j - \bar{x}\,, \qquad p_j = u_j - \bar{u} \tag{105}$$

be the relative coordinates with respect to the center of mass. Substituting Eq. (105) into Eq. (1) we have

$$\frac{dq_j}{dt} = p_j\,, \qquad \frac{dp_j}{dt} = -\left(2a\,\cos\bar{x}\right)\,q_j\ . \tag{106}$$

Approximating $\bar{x} \approx 0$, and using the mean field equation, we conclude that the relative position evolves according to the Mathieu equation

$$\frac{d^2 q_j}{d\hat{\tau}^2} + \left[1 + 2\left(\frac{5+9\lambda}{3}\right)\,\varepsilon^2\ - 2\,\varepsilon\,\cos\hat{\tau}\right]\,q_j = 0\,. \tag{107}$$

The stability properties of this Mathieu equation are well-understood. In particular, the equilibrium solution $(q, dq/d\hat{\tau}) = (0,0)$ is stable if $\lambda > 5/9$ and unstable if $\lambda < 5/9$; see for example Ref. [22]. In terms of the parameter α, the dynamics of the relative coordinates is stable if and only if

$$\alpha > \alpha_b = (5/6)^{2/3}\,. \tag{108}$$

Figure 8 illustrates this transition.

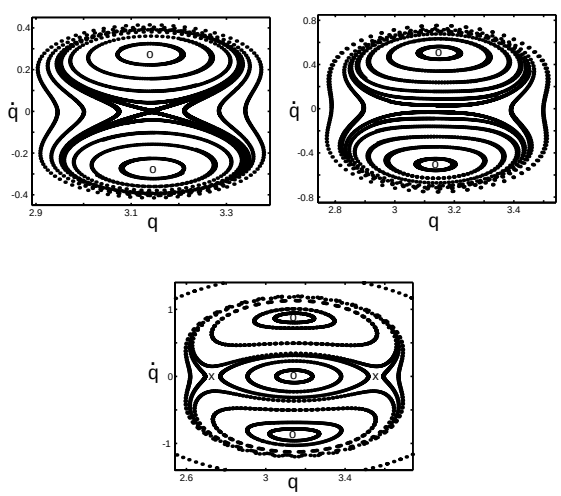

Fig. 8. Poincare sections in the $(q_j, \dot{q}_j)$ –plane of Eq. (107), illustrating the bifurcation of the stability properties of the origin due to parametric resonance. In (a) $\alpha = 2$, and in (c) $\alpha = 0.2$. Panel (b) corresponds to the bifurcation point $\alpha = \alpha_b = (5/6)^{2/3} = 0.8855$ according to Eq.(108). To ease the comparison with the Fig. 7, we have shifted $q_j \to q_j + \pi$.

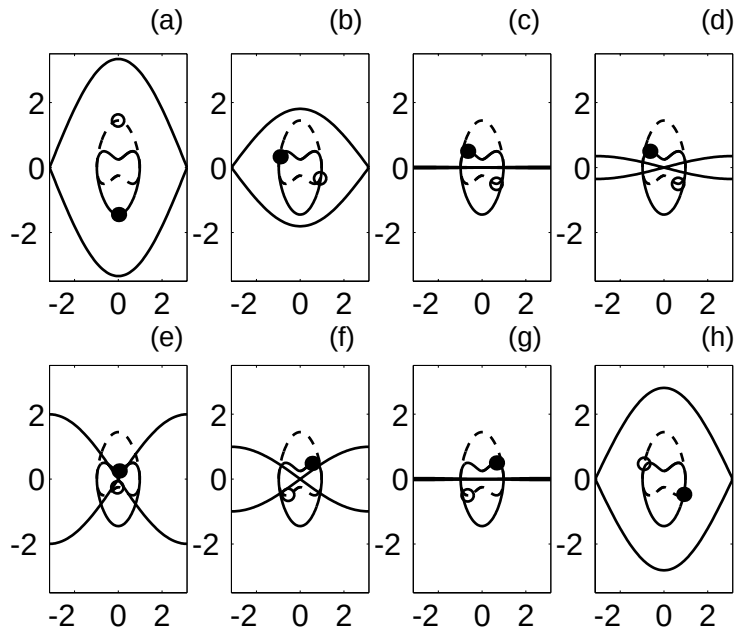

Fig. 9. Elliptic-hyperbolic bifurcation generated by a trapped $N = 2$ rotating hole-clump system.

8 Violent mixing

The SWM Hamiltonian for a symmetric state

$$H = \sum_{j=1}^{N} \left[\frac{u_j}{2} - 2a(t)\, \cos x_j \right] , \tag{109}$$

has fixed points at $(x_j, u_j) = (0, 0)$ and $(\pi, 0)$. The stability of these fixed points depends on the sign of the mean field a. If $a > 0$, $(0, 0)$ is stable (elliptic) and $(\pi, 0)$ is unstable (hyperbolic). However, if $a < 0$, $(0, 0)$ is unstable (hyperbolic) and $(\pi, 0)$ is stable (elliptic). Thus, a change in the sign of a implies an elliptic-hyperbolic bifurcation. An example of this bifurcation is illustrated in Fig. 9 where we have plotted the evolution of an $N = 2$ hole-clump pair together with the instantaneous location of the separatrix of the Hamiltonian in phase space. Because of the mean field nature of the model, it is irrelevant which phase space plane one chooses because (x_k, u_k) evolves under the same Hamiltonian for all k. As the hole-clump rotates, the width of the separatrix decreases and eventually vanishes. At this point, panel (c), an elliptic-hyperbolic bifurcation occurs leading to the creation of an hyperbolic point at the origin as shown in panel (d). As the hole-clump rotates the separatrix grows, and once again eventually decreases and vanishes, leading to another bifurcation that restores

the elliptic point at the origin. In this case, this sequence of bifurcations repeats indefinitely because the mean-field is periodic and changes sign twice during one rotation period of the dipole.

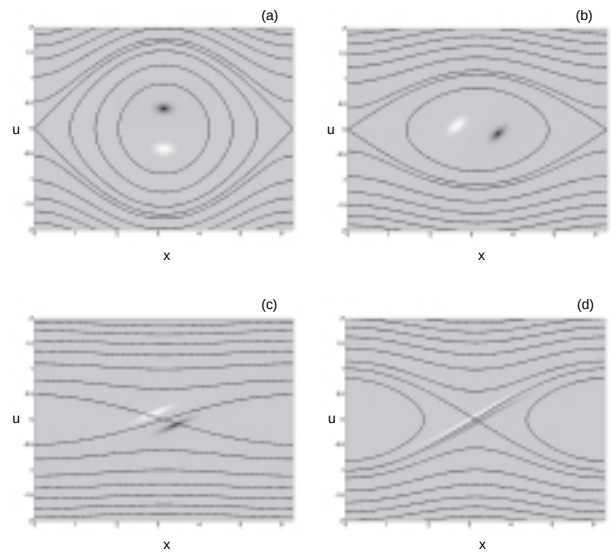

Fig. 10. Dipole destruction due to mean-field elliptic-hyperbolic bifurcation.

An elliptic-hyperbolic bifurcation occurs whenever the mean field vanishes. Whether or not this happens during the evolution of the system depends on the initial conditions and the parameter values of the system. The symmetric $N = 2$ system is particularly simple to understand. As discussed previously, this system is integrable, and the clump orbits follow the iso-contours of the nontwist Hamiltonian (36) in the (x, A) space shown in Fig. 2. In this case, the orbits that exhibit elliptic-hyperbolic bifurcations are those that cross the $A = 0$ dashed line. Consider an orbit with initial condition (x_0, u_0) that exhibits an elliptic-hyperbolic bifurcation when it is at (x_b, u_b). Because the Hamiltonian is a constant of motion, $H = \alpha A_0 - A_0^3/3 + \cos x_0 = \cos x_b$. Using the fact that $-1 < \cos x_b < 1$, we get the following condition for the bifurcation to occur [14]:

$$-1 < \alpha\, A_0 - \frac{A_0^3}{3} + \cos x_0 < 1\,. \tag{110}$$

Assuming for the sake of simplicity that $x_0 = 0$ and using the definition of α in (37) we can write this condition as in terms of the initial conditions $a_0 = a(0)$, $u_0 = u(0)$, and the value of Γ

$$-6\,\Gamma^2 < 3\,\Gamma u_0\, a_0 + 2\, a_0^3 < 0\,. \tag{111}$$

In the case $N \gg 1$, and in the kinetic limit, the elliptic-hyperbolic bifurcation can lead to the destruction of phase space coherent structures. For example,

panel (a) in Fig. 10 shows the initial condition in Eq. (95) consisting of two symmetric Gaussian-distributed holes and clumps with $\gamma = 12$, $x_1 = \pi$, $x_2 = \pi$, $u_1 = -u_2 = -0.4$, and $a_0 = -0.36$. This is the same initial condition as the one used in Fig. 4 except that the value of γ has been increased. Note also that the dipole in Fig. 10-(a) is rotated by π, and that there is a corresponding phase shift in $a(t)$. At the beginning the dipole rotates around $(x, y) = (\pi, 0)$, but eventually an elliptic-hyperbolic bifurcation occurs and the dipole is destroyed and filaments along the unstable manifolds of the hyperbolic point. At this point, to follow the evolution of this system, it is more convenient to resort to finite–N particle simulations. In these simulations, it is observed that the dipole filamentation due to the elliptic–hyperbolic bifurcation is followed by the chaotic mixing of the holes and clumps in the stochastic layer of the mean field [14].

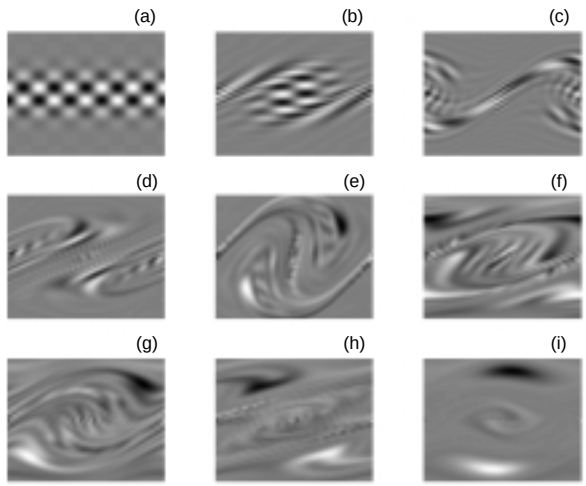

Fig. 11. Violent relaxation of far from equilibrium initial condition. The different panels, show the phase space at $t = 0$, 2.5, 5, 10, 17.5, 30, 32.5, 40, 100.

Hyperbolic-elliptic bifurcations can occur in more general settings and they lead to a very rapid mixing of far from equilibrium initial conditions. An example is shown in Fig. 11 where, after several successive elliptic-hyperbolic bifurcations, the system relaxes to a coherent state consisting of two untrapped dipoles traveling in opposite directions. In this case, the mean field, shown in Fig. 12, vanishes several times during a transient phase, and then it relaxes to a near periodic state. The relaxation of far from equilibrium states in systems with long-range interactions is a problem of interest in hydrodynamics, plasmas and galactic dynamics, and several models have been discussed in the literature as potential mechanisms. The elliptic-bifurcation discussed above is a novel mixing

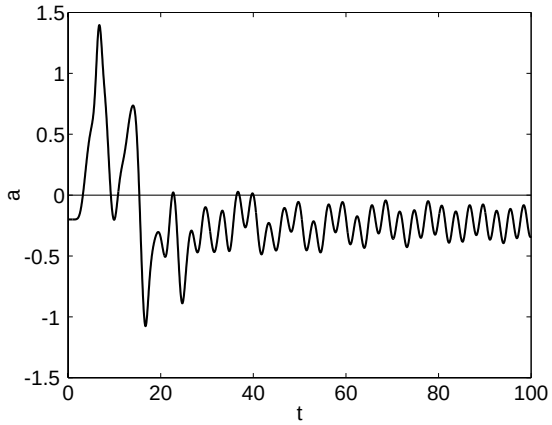

Fig. 12. Mean field $a(t)$ corresponding to the simulation in Fig. 11. The vanishing of a gives rise to elliptic-hyperbolic bifurcations in the phase space.

mechanism which in the SWM leads to "violent relaxation". We use here the term violent relaxation (a term originally introduced in galactic dynamics) to distinguish this kind of mixing from other milder phase space mixing mechanisms including phase mixing and chaotic mixing.

9 Conclusions

We have presented a study of the single wave model which is a mean field Hamiltonian model that describes the weakly nonlinear dynamics of fluids and plasmas. The relative mathematical simplicity of the model makes it a tractable system to study the dynamics of large degrees-of-freedom, long-range interacting systems. Understanding the coexistence of coherent structures and self-consistent Hamiltonian chaos is a problem of interest to fluid dynamics, plasma physics, galactic dynamics, and statistical mechanics. Two-dimensional, incompressible fluids and plasmas are known to develop large–scale coherent structures that live in a turbulent background. From a dynamical systems point of view, the problem is to explain the self-consistent formation of islands of integrability that shield the coherent structures from the chaotic mixing of the background. In this chapter we have shown that in the SWM there is a self-consistent parametric resonance between the rotation frequency of the dipole and the frequency of the mean field. This resonance creates islands of stability that shield the dipole from the chaotic transport of the background. A problem complementary to the formation of coherent structures is the problem of "violent" mixing and relaxation of far from equilibrium initial conditions. We have shown that in the SWM the mean field can exhibit hyperbolic-elliptic bifurcations in the phase space that lead to very rapid or "violent" mixing of phase space structures. By "violent " we mean that the time scale of the mixing is faster than a diffusive or chaotic advection mixing

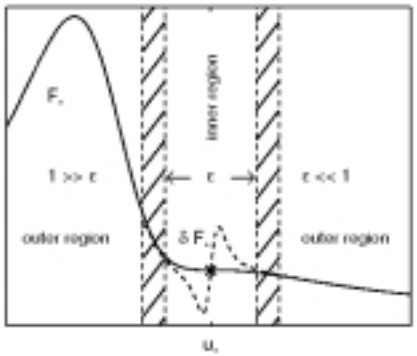

Fig. 13. Sketch of a localized perturbation (dashed line) on a marginally stable equilibrium (solid line). The matched asymptotic expansion discussed in the appendix reduces the Vlasov-Poisson system (9)–(10) to the single wave model (6)–(8) that describes the nonlinear evolution in the inner, $O(\varepsilon)$, region. In the outer, $1 \gg \varepsilon$, region the system responds linearly. The shaded area is the asymptotic matching region [11].

process. We also discussed the linear stability of equilibria and the problem of Landau damping in the kinetic limit of the single wave model.

Acknowledgments

I would like to give special thanks to my collaborator in the study of self-consistent chaos and coherent structures, Marie-Christine Firpo. Also, it is a pleasure to acknowledge useful conversations with P. J. Morrison, A. Vulpiani, G. Boffetta, S. Ruffo, and Y. Elskens. Finally, I want to thank the organizers of the Les Houches Winter School, Thierry Dauxois, Stefano Ruffo, Ennio Arimodo, and Martin Wilkens for inviting me to participate in a very enlightening workshop that, hopefully, will promote a long-range interaction among its participants. This work was sponsored by the Oak Ridge National Laboratory, managed by UT-Battelle, LLC, for the U.S. Dept. of Energy under contract DE-AC05-00OR22725.

Appendix A: Derivation of the SWM for marginally stable Vlasov-Poisson systems

In this appendix we derive the single wave model in Eqs. (6)-(8) as a weakly nonlinear description of Vlasov-Poisson systems of the form in Eqs. (9)-(10). We skip technical details that the interested reader can find in Refs. [10,11].

The starting point is the assumption that the equilibrium is marginally stable with a stationary inflexion point at $u = c_0$, that is $F_0'(c_0) = F_0''(c_0) = 0$. The destabilization of F_0 is caused by perturbations that turn the locally flat region around the stationary inflection point into a region of adverse gradient as shown in Fig. 13.

We introduce the slow time variable

$$t \equiv (2\pi/L)\,\varepsilon\,T \ , \tag{112}$$

where ε, the small parameter of the perturbation expansion, is proportional to the growth rate of the instability, and L is the spatial length of the system. The quantization condition implies

$$k = \frac{2\pi}{L} = k_0(1 - \varepsilon\Lambda) \ , \tag{113}$$

where k is the wavelength of the instability, k_0 is the wavelength of the neutral inflexion point mode, and Λ is a constant. In addition, we assume the trapping scaling according to which the amplitude of the nonlinear saturated fields is of order ε^2,

$$F = \varepsilon^2\, f\,(x, u, t) \ , \qquad \Phi = \varepsilon^2\, \phi\,(x, t)\,, \tag{114}$$

and do a Galilean transformation to a reference frame moving at the speed of the inflection point mode

$$x \equiv (2\pi/L)(X - c_0 T) \ . \tag{115}$$

In terms of the variable x, the domain has period 2π, and ϕ, and f can be expanded as a Fourier series:

$$\phi(x,t) = \sum_{n=-\infty}^{\infty} \tilde{\phi}(n,t)\, e^{inx} \ , \qquad f(x,u,t) = \sum_{n=-\infty}^{\infty} \tilde{f}(n,u,t)\, e^{inx} \ . \tag{116}$$

Substituting Eqs. (112)–(116) into Eq. (9) and Eq. (10) we get

$$\varepsilon\,\partial_t f + (u - c_0)\,\partial_x f + \left(F_0' + \varepsilon^2 \partial_u f\right)\,\partial_x \phi = 0 \ , \tag{117}$$

$$G\left[n k_0\,(1 - \varepsilon\Lambda)\right]\tilde{\phi}(n,t) = -\int_{-\infty}^{\infty} \tilde{f}(k,u,t) du \ . \tag{118}$$

These equations are exact, and the derivation of the SWM proceeds by a perturbative solution of them.

In the perturbation expansion, we write

$$\phi(x,t) = \phi_0 + \varepsilon\,\phi_1 \ldots \tag{119}$$

and divide the (x,u) space in two regions; an inner region where $u - c_0 = O(\varepsilon)$ and an outer region where $u - c_0 = O(1)$. In each region we solve Eq. (117) by expanding f in powers of ε and match the solution in the intermediate region. Once a global solution of f is found, ϕ is determined self-consistently from Eq. (118).

To treat the inner region, we introduce the stretched coordinate $v = (u - c_0)/\varepsilon$, substitute $f = f_0^i + \varepsilon f_1^i + \ldots$ into Eq. (117), and get at first order a Vlasov equation describing the distribution function in the inner region

$$\partial_t f_0^i + v\partial_x f_0^i + \partial_x\phi_0\,\partial_v f_0^i = 0\,. \tag{120}$$

In the outer region, $u - c_0 = O(1)$, we substitute $\tilde{f}(n,u,t) = \tilde{f}_0^o + \varepsilon\,\tilde{f}_1^o + \ldots$ into Eq. (117) and get at $O(1)$ the linear eigenmode of the instability

$$\tilde{f}_0^o = -\frac{F_0'}{u - c_0}\,\tilde{\phi}_0 \tag{121}$$

and at $O(\varepsilon)$

$$\tilde{f}_1^o = -\frac{i}{n}\,\frac{F_0'}{(u-c_0)^2}\,\partial_t\tilde{\phi}_0 - \frac{F_0'}{u - c_0}\,\tilde{\phi}_1\,. \tag{122}$$

Note that, because of the inflexion point condition $F_0'(c_0) = F_0''(c_0) = 0$, there are no singularities in Eqs. (121)-(122). The last step in the derivation is to derive a self-consistent equation for the potential by solving Eq. (118) perturbatively. At $O(1)$ Eq. (118) reduces to the dispersion relation of the neutral model, and at $O(\varepsilon)$

$$G\,(nk_0)\;\tilde{\phi}_1 - nk_0\Lambda\,G'\,(nk_0)\;\tilde{\phi}_0 = -\int_{-\infty}^{\infty}\tilde{f}_1^o\,du - \int_{-\infty}^{\infty}\tilde{f}_0^i\,dv\;. \tag{123}$$

Because $\int \tilde{f}^i du = \varepsilon \int \tilde{f} dv$, the zeroth order term in the inner field, f^i, contributes to the first order term of ϕ. Substituting (121) into (123), we conclude $n = \pm 1$, and

$$\phi_0 = \tilde{\phi}_0(1,t)\,e^{ix} + \tilde{\phi}_0(-1,t)\,e^{-ix}\;. \tag{124}$$

That is, the single-wave spatial structure of the potential arises naturally from the leading order balance in (118). To determine the time evolution of ϕ_0, we substitute (121) into (123) and get

$$\gamma\,\frac{d\tilde{\phi}_0}{dt} + i\lambda\,\tilde{\phi}_0 = \frac{i}{2\pi}\int_{-\infty}^{\infty}\int_0^{2\pi} e^{-ix} f_0^i\,dxdv\;. \tag{125}$$

Equations (120) and (125) form a closed, self-consistent system of equations describing the nonlinearly saturated state in the vicinity of the stationary inflection point. Defining $\sigma \equiv \mathrm{sign}\,(\gamma)$, $\ell \equiv \mathrm{sign}\,(\Lambda)$ where "sign" denotes the sign, and $\mathrm{sign}\,(0) = 0$, and rescaling as $v \to |\lambda/\gamma|\;v$, $t \to |\gamma/\lambda|\;t$, $f \equiv |\gamma|/\lambda^2\;f_0^i$, $a \equiv (\gamma/\lambda)^2\;\tilde{\phi}_0$, Eqs. (120) and (125) become the SWM in (6)-(8).

References

1. M. Antoni, Y. Elskens, and D. F. Escande, Phys. Plasmas **5**, 841 (1998)
2. M. Antoni and S. Ruffo, Phys. Rev. E **52**, 2361 (1995)
3. N. J. Balmforth, D. del-Castillo-Negrete, and W. R. Young, J. Fluid Mech., **333**, 197-230 (1997).
4. N. J. Balmforth, S. L. Smith and W. R. Young, J. Fluid Mech., **10**, 95-133 (2001).
5. N. J. Balmforth and C. Piccolo, J. Fluid Mech. **449**, 85-114 (2001).
6. J. Barre, T. Dauxois, and S. Ruffo, Physica A **295**, 254-60 (2001).
7. H. L. Berk, B. N. Breizman, et. al., Phys. Plasmas **6**, 3102 (1999).
8. S. M. Churilov, and G. Shukhman, Astrophys. Fluid Dynamics, **38**, 145 (1987)
9. J. D. Crawford and A. Jayaraman, Phys. Plasmas **6**, (1999).
10. D. del-Castillo-Negrete, Phys. Lett. A **241**, 99 (1998).
11. D. del-Castillo-Negrete, Phys. Plasmas **5**, 3886 (1998).
12. D. del-Castillo-Negrete, Physica A **280**, 10 (2000).
13. D. del-Castillo-Negrete, Chaos **10**, 75 (2000).
14. D. del-Castillo-Negrete and M.-C. Firpo, Chaos **12**, 496 (2002).
15. D. del-Castillo-Negrete, J. M. Greene and P. J. Morrison, Physica D **91**, 1 (1996).
16. T. Dauxois, V. Latora, A. Rapisarda, S. Ruffo and A. Torcini, *The Hamiltonian Mean Field Model: from Dynamics to Statistical Mechanics and back*, in "Dynamics and Thermodynamics of Systems with Long Range Interactions", T. Dauxois, S. Ruffo, E. Arimondo, M. Wilkens Eds., Lecture Notes in Physics Vol. 602, Springer (2002), (in this volume)
17. D. F. Escande, S. Zekri and Y. Elskens, Phys. Plasmas **3**, 3534 (1996).
18. D. Farina, F. Casagrande, U. Colombo, R. Pozzoli, Phys. Rev. E, **49**, 1603 (1994).
19. M.-C. Firpo and Y. Elskens, J. Stat. Phys. **93**, 193 (1998)
20. M.-C. Firpo and Y. Elskens, Phys. Rev. Lett. **84**, 3318 (2000).
21. M. E. Goldstein, and L. S. Hultgren, J. Fluid Mech. **197**, 295 (1988).
22. E. J. Hinch, *Perturbation Methods*, Cambridge University Press, New York, (1991).
23. L. Landau, J. Phys. USSR (Moscow) **10**, 85-93 (1946).
24. V. Latora, A. Rapisarda, and S. Ruffo, Physica D, **131**, 38 (1999).
25. A. J. Lichtenberg, and M.A. Lieberman, *Regular and stochastic motion*, Springer-Verlag, second edition (1983).
26. D. R. Nicholson, *Introduction to Plasma Theory*, Wiley (1983).
27. T. M. O'Neil, J. H. Winfrey and J. H. Malmberg, Phys. Fluids **14**, 1204 (1971).
28. I. N. Onischenko *et al.*, JETP Lett. **12**, 281 (1970).
29. J. L. Tennyson, J. D. Meiss and P. J. Morrison, Physica D **71** , 1 (1994).
30. H. Weitzner, Phys. Fluids **6**, 1123-1127 (1963).